Searches for supersymmetry with the ATLAS detector

Abhishek Sharma

abhishek@cern.ch

DIS 2021

THE UNIVERSITY *of* ADELAIDE

ATLAS EXPERIMENT

Supersymmetry at ATLAS

- ATLAS has a strong and varied supersymmetry (SUSY) search program!
  - Strong SUSY: squark and gluino production
  - Electroweak: chargino, neutralino, sleptons
  - RPV and long-lived: specialised techniques and rare signatures
  - Summaries and combinations: putting everything together
- Today I will cover four recently released analyses

SUSY model classification

There are a wide range of possible model parameters and final states to probe:

- R-parity conservation (RPC) or violation (RPV)
- Wino-bino or higgsino dominated electroweak processes
- Symmetry breaking scenarios: different LSPs, mass hierarchies etc
- Different kinematic regimes depending on masses and couplings!

Search for new phenomena in *pp* collisions in final states with tau leptons, *b*-jets, and missing transverse momentum with the ATLAS detector

ATLAS-CONF-2021-008

Motivation and models

- Two benchmark models considered:
  - Gauge mediated SUSY with the stop, stau, and gravitino LSP
  - Scalar leptoquark production with decays to 3$^{\mathrm{rd}}$ generation SM quark and lepton pairs
- For the SUSY model, the squarks decay to the gravitino LSP via a stau with *b*-jets, tau leptons and neutrinos
- The leptoquarks are charge 1/3 or 2/3 with decays to $t\nu$ or $b\tau$ final states

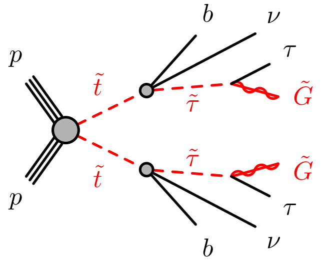

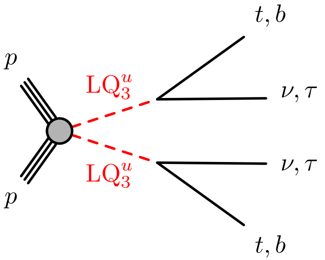

Analysis strategy

Signal regions

- $E_{\mathrm{T}}^{\mathrm{miss}}$ trigger fired with at least 250 GeV $E_{\mathrm{T}}^{\mathrm{miss}}$
- No light leptons
- At least two jets
- At least one b-jet
- Two complimentary channels:
  - Di-tau with at least two hadronic tau candidates
  - Single-tau with one tau and at least two b-jets, split into bins based on tau p_{T}
- Discriminating variables are m_{T2} and sums of object masses

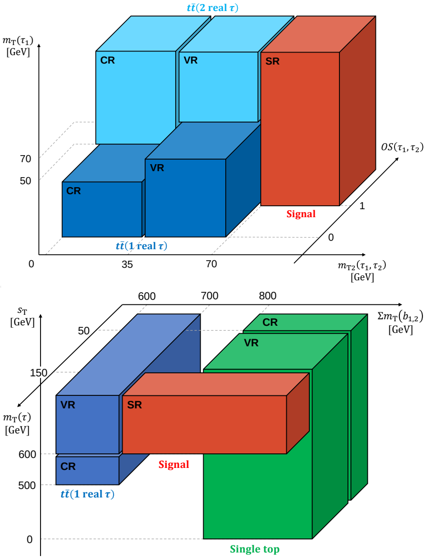

- $t\bar{t}$ and single top with 1 or 2 real taus + fakes → dedicated CRs and VRs
- Smaller contributions from V+jets, $t\bar{t}V$
- Major uncertainties from jet energy resolution, modelling, and $t\bar{t}/Wt$ interference

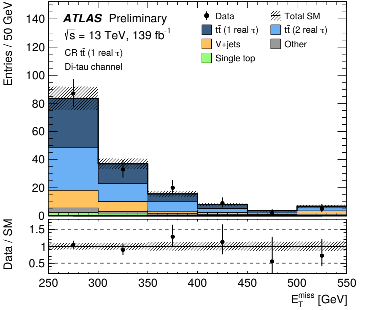

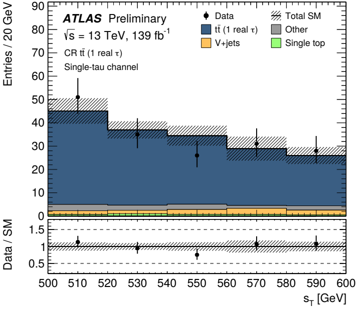

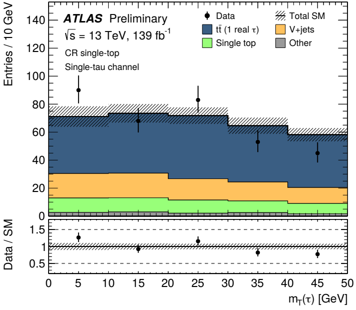

Results and limits

- No significant excesses
- Single tau SR is new for full Run 2 dataset, and markedly improves sensitivity
- Good improvement from previous analyses for stop to stau model
- Leptoquark models discussed in Stergios' talk

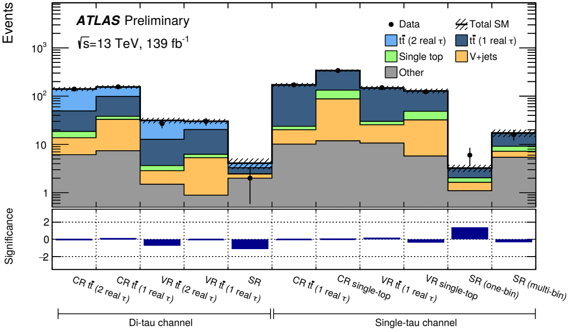

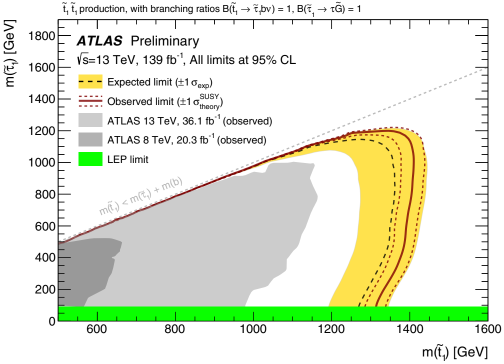

Search for R-parity violating supersymmetry in a final state containing leptons and many jets with the ATLAS experiment using $\sqrt{s} = 13$ TeV proton-proton collision data

ATLAS-CONF-2020-007

- RPV models with both strong and electroweak production
- Either direct decays to LSP or via an intermediary
- Large numbers of jets and at least one light lepton

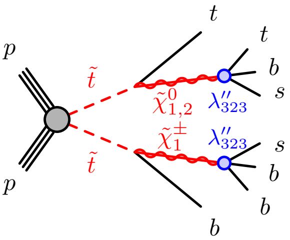

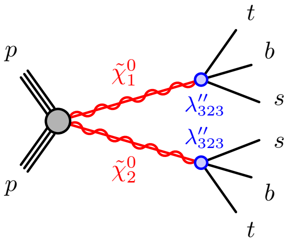

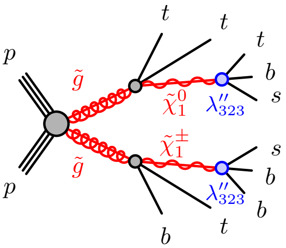

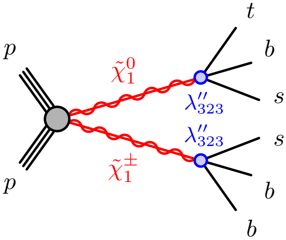

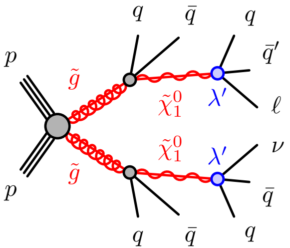

Analysis strategy

- Two strategies: a generic jet counting analysis, and an electroweak analysis with a neural net discriminant
- Further split by lepton content: 1 lepton (1ℓ) or 2 same-charge leptons ($2\ell^{\mathrm{SC}}$)
- Events must pass single lepton trigger, and di-electron events have a Z mass veto
- Jet counting analysis has a range of jet momentum thresholds to maximise sensitivity

Jet counting analysis discovery SRs			
Jet p_{T} threshold	Number of jets 1ℓ category	Number of jets $2\ell^{\mathrm{sc}}$ category	Number of b-jets
20 GeV	≥ 15	≥ 10	$= 0, \geq 3$
40 GeV	≥ 12	≥ 8	$= 0, \geq 3$
60 GeV	≥ 11	≥ 7	$= 0, \geq 3$
80 GeV	≥ 10	≥ 7	$= 0, \geq 3$
100 GeV	≥ 8	≥ 6	$= 0, \geq 3$

EWK analysis discovery SRs			
Jet p_{T} threshold	Lepton category and selection	Number of jets	Number of b-jets
20 GeV	1ℓ, NN bin 4	$= 6$	≥ 4
20 GeV	$2\ell^{\mathrm{sc}}$, $m^{\ell j} < 155$ GeV	$= 6$	≥ 3

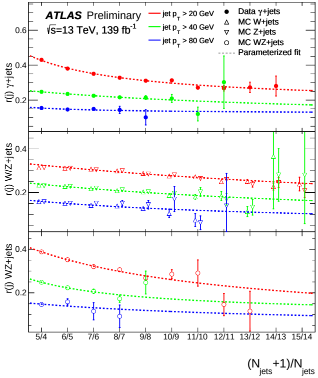

- Data driven estimation of $t\bar{t}$, $t\bar{t}V$, V+jets, VV+jets
- Using probability of extra (b-)jets to fit a functional form for each jet multiplicity
- The fit is tested using γ+jets and dileptonic $t\bar{t}$
- Fake backgrounds in the 1ℓ category is from Matrix Method

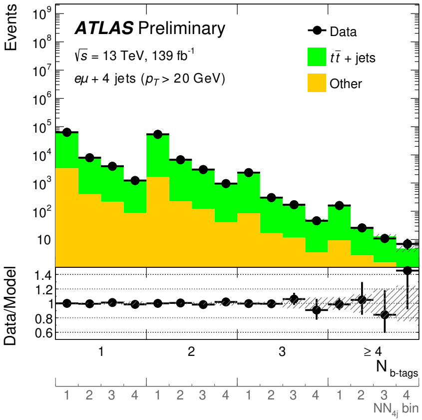

Dominant uncertainties come from (b-)jet scaling assumptions, b content of $V(V)$ MC, and NN response

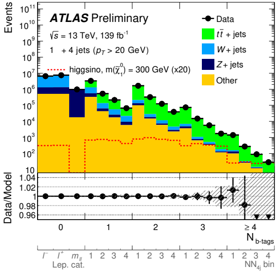

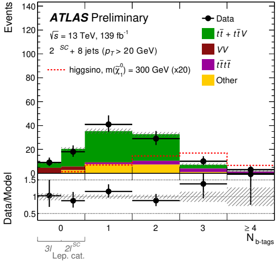

No significant excesses

- Good data/bkg agreement across all regions, even those with high jet multiplicity
- Largest deviation in two bins with 1.3σ

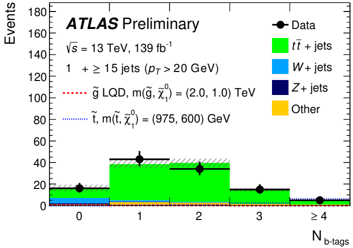

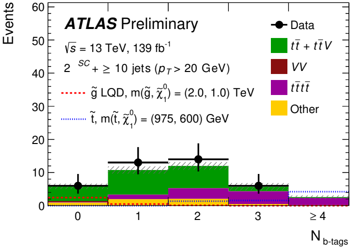

- This analysis is also sensitive to 4 top production!
- Extracted signal strength $\mu = 2.0^{+0.9}_{-0.7}$
- This is comparable to recent results from ATLAS in 1, 2, and 3 lepton channels
- 1 ℓ and opposite-charge 2ℓ, and same-charge 2ℓ and 3 ℓ

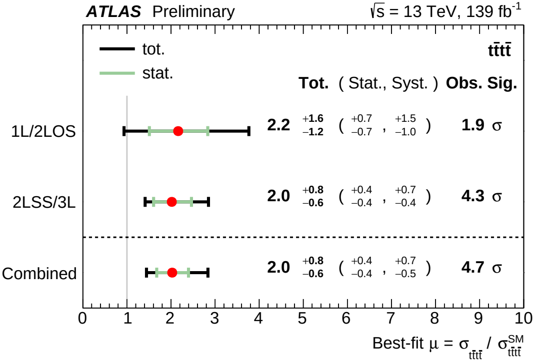

Model dependent limits

- Exclusion for up to 2.2 TeV gluinos for multiple decay channels
- LSP type changes the expected exclusion due to different final states
- Higgsino versus wino LSP hypotheses in the electroweak models changes exclusion
- First LHC result for Higgsinos in the hadronic final state

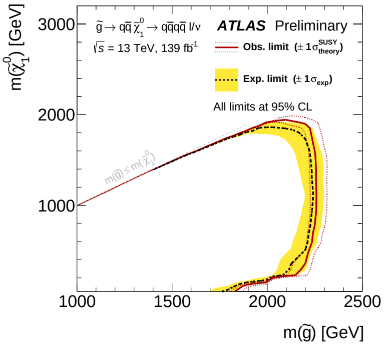

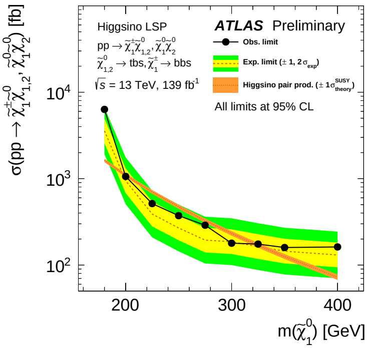

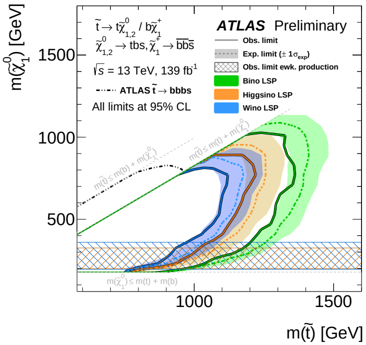

Search for stopped long-lived charginos based on a disappearing-track signature using 136 fb^{-1} of pp collisions at $\sqrt{s} = 13$ TeV with the ATLAS detector

ATLAS-CONF-2021-015

Motivation and models

- In certain SUSY models with electroweak scale LSPs the mass difference between $\tilde{\chi}_1^0$ and $\tilde{\chi}_1^\pm$ is around 100 MeV
- This leads to charginos with decay length in the mm range:

$$c\tau[\mathrm{mm}] \sim 7 \times \left[\left(\frac{\Delta m(\tilde{\chi}_1^\pm, \tilde{\chi}_{1,2}^0)}{340\mathrm{MeV}} \right)^3 \sqrt{1 - \frac{m_{\pi^\pm}^2}{\Delta m(\tilde{\chi}_1^\pm, \tilde{\chi}_{1,2}^0)^2}} \right]^{-1},$$

  where $m_{\pi^\pm}$ is the charged pion mass
- Look for pixel tracklets without other significant activity in outer detector layers
- This analysis looks at electroweak and strong production modes

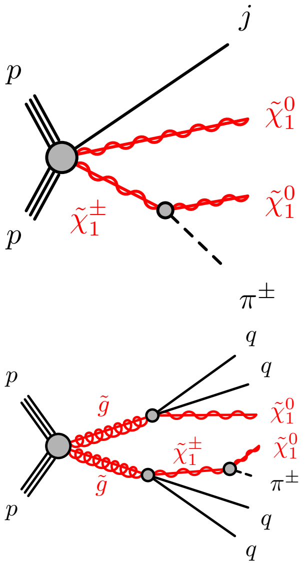

Analysis strategy

- Only record hits in pixel tracking layers
- Veto pixel tracklets with associated calorimeter deposits > 5 GeV
- Use missing energy triggers with dedicated efficiency measurement
- Require large $E_{\mathrm{T}}^{\mathrm{miss}}$, ≥ 1 (electroweak) or ≥ 3 jets with the leading jet ≥ 100 GeV

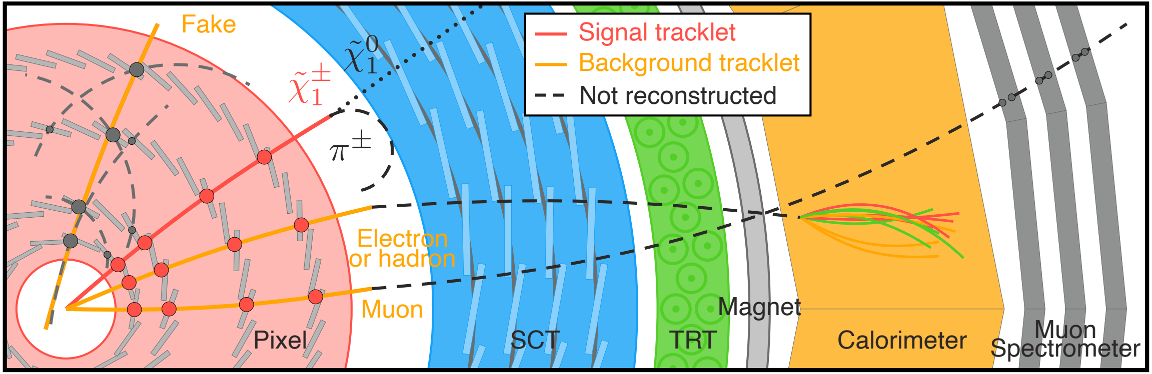

Background estimation

- Charged particle scattering and combinatorial fakes are the two main backgrounds
- Design CRs with background templates for electron, muon, hadron, and fakes
- Also use low $E_{\mathrm{T}}^{\mathrm{miss}}$ CR, and medium $E_{\mathrm{T}}^{\mathrm{miss}}$ VRs
- Develop fit model to fit low, medium and high $E_{\mathrm{T}}^{\mathrm{miss}}$ simultaneously to determine SR backgrounds

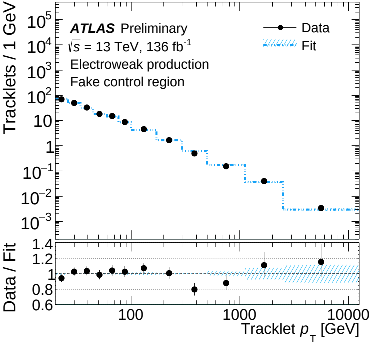

The fit model encodes the systematics, with pile-up and fake tracklet CR uncertainties being the major contributors
Cross-section calculations, ISR/FSR, and tracklet reconstruction uncertainties affect the signal yields

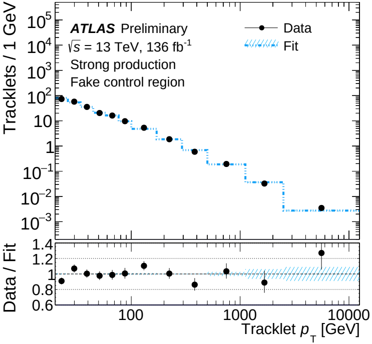

Results and limits

- No significant excess
- Able to reach short lifetimes and large masses for both wino and higgsino scenarios
- Probing new parameter space for strong production too

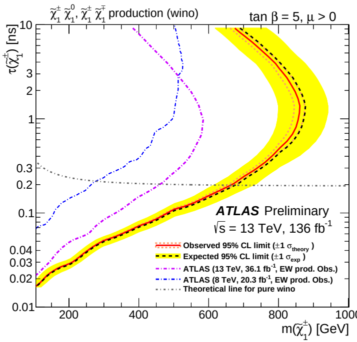

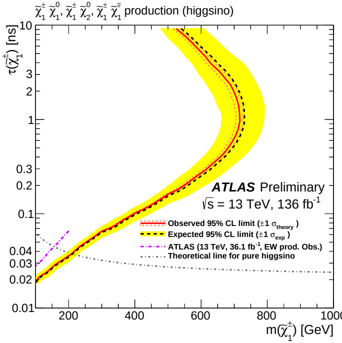

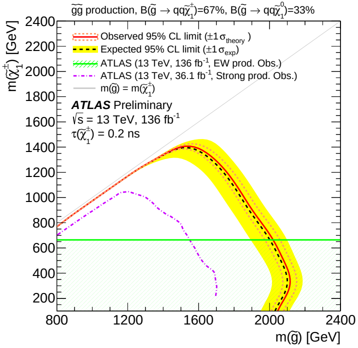

A search for the decays of stopped long-lived particles at $\sqrt{s} = 13$ TeV with the ATLAS detector

SUSY-2018-15

- If long-lived gluinos are produced and slow down enough as they pass through the detector, they can bind with SM particles to form *R*-hadrons
- These *R*-hadrons can then decay at a later time
- A range of masses and mass splittings are simulated

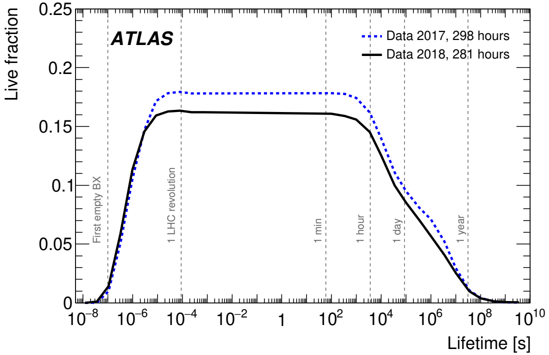

The signal MC generation has been discussed in detail in

ATL-PHYS-PUB-2019-019

Analysis strategy

- Use empty bunch crossings (BX): special triggers and separate dataset in 2017 and 2018!
- Expect isotropic decays to jets from anywhere in the detector
- Two broad SRs: one covering central η and another up to $|\eta| < 2.4$
- Require at least one energetic jet with regions binned in (150-300, 300-500, >500) GeV lead jet momentum

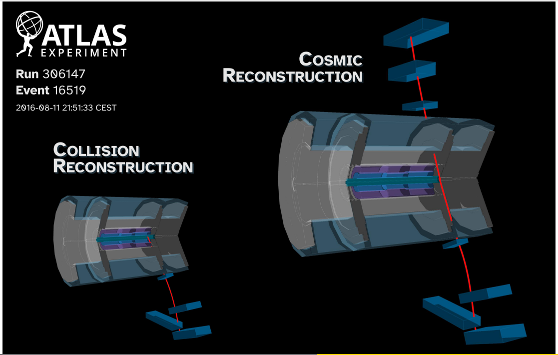

Need to have cosmic reconstruction instead of usual collision reco to properly veto backgrounds

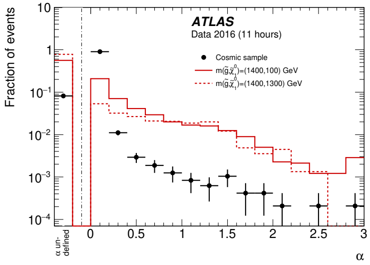

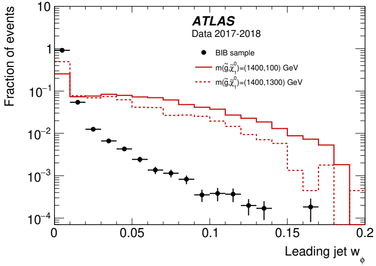

- Major backgrounds are cosmic muons and beam induced backgrounds (BIB)
- Use special variables α (distance between jet and bkg muon), and $w_\phi = \frac{\sum_i p_{\mathrm{T}}(i) \cdot |\Delta\phi(\mathrm{jet}, i)|}{\sum_i p_{\mathrm{T}}(i)}$ (to suppress BIB)
- Control and validation regions for the two background sources

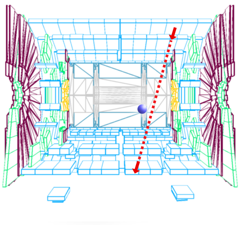

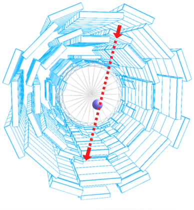

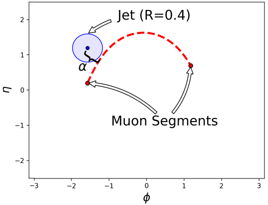

- No significant excess
- Reach up to 1400 GeV for a wide range of lifetimes
- Smaller mass splitting has lower sensitivity
- Time range from one bunch crossing to a year

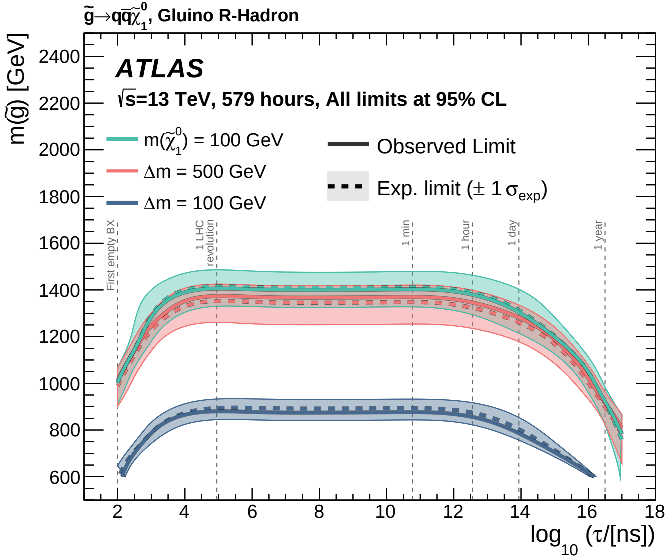

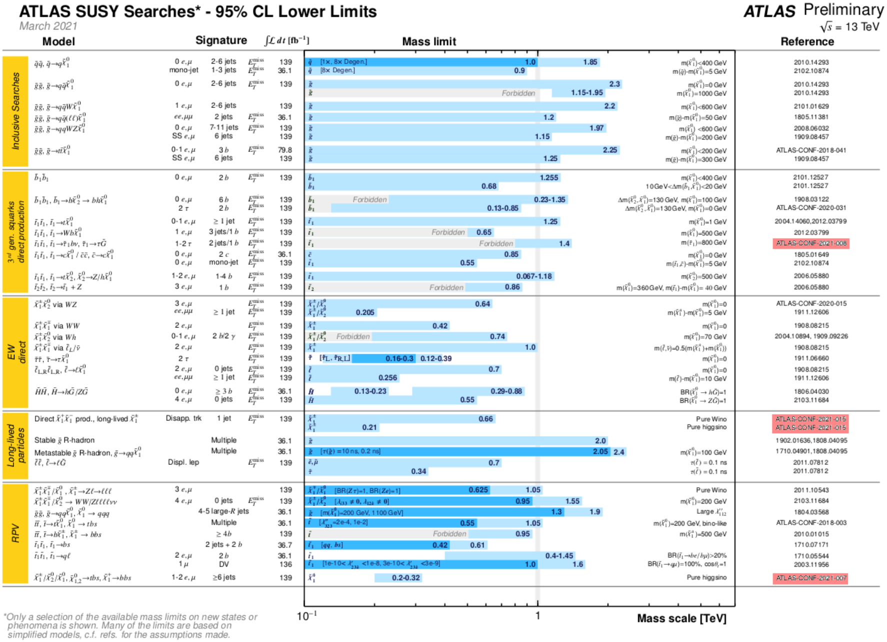
ATLAS SUSY Searches* - 95% CL Lower Limits
March 2021
ATLAS Preliminary
$\sqrt{s}$ = 13 TeV
Model
Signature
$\int \mathcal{L}\, dt$ [fb^{-1}]
Mass limit
Reference
Inclusive Searches
$\tilde{q}\tilde{q}$, $\tilde{q}\to q\tilde{\chi}_1^0$ | 0 e,μ | 2-6 jets | E_T^{miss} | 139 | $\tilde{q}$ [1×, 8× Degen.] 1.0 1.85 | m($\tilde{\chi}_1^0$)<400 GeV | 2010.14293
mono-jet | 1-3 jets | E_T^{miss} | 36.1 | $\tilde{q}$ [8× Degen.] 0.9 | m($\tilde{q}$)-m($\tilde{\chi}_1^0$)=5 GeV | 2102.10874
$\tilde{g}\tilde{g}$, $\tilde{g}\to q\bar{q}\tilde{\chi}_1^0$ | 0 e,μ | 2-6 jets | E_T^{miss} | 139 | $\tilde{g}$ 2.3 | m($\tilde{\chi}_1^0$)=0 GeV | 2010.14293
$\tilde{g}$ Forbidden 1.15-1.95 | m($\tilde{\chi}_1^0$)=1000 GeV | 2010.14293
$\tilde{g}\tilde{g}$, $\tilde{g}\to q\bar{q}W\tilde{\chi}_1^0$ | 1 e,μ | 2-6 jets | 139 | $\tilde{g}$ 2.2 | m($\tilde{\chi}_1^0$)<600 GeV | 2101.01629
$\tilde{g}\tilde{g}$, $\tilde{g}\to q\bar{q}(\ell\ell)\tilde{\chi}_1^0$ | $ee,\mu\mu$ | 2 jets | E_T^{miss} | 36.1 | $\tilde{g}$ 1.2 | m($\tilde{g}$)-m($\tilde{\chi}_1^0$)=50 GeV | 1805.11381
$\tilde{g}\tilde{g}$, $\tilde{g}\to qqWZ\tilde{\chi}_1^0$ | 0 e,μ | 7-11 jets | E_T^{miss} | 139 | $\tilde{g}$ 1.97 | m($\tilde{\chi}_1^0$) <600 GeV | 2008.06032
SS e,μ | 6 jets | 139 | $\tilde{g}$ 1.15 | m($\tilde{g}$)-m($\tilde{\chi}_1^0$)=200 GeV | 1909.08457
$\tilde{g}\tilde{g}$, $\tilde{g}\to t\bar{t}\tilde{\chi}_1^0$ | 0-1 e,μ | 3 b | E_T^{miss} | 79.8 | $\tilde{g}$ 2.25 | m($\tilde{\chi}_1^0$)<200 GeV | ATLAS-CONF-2018-041
SS e,μ | 6 jets | 139 | $\tilde{g}$ 1.25 | m($\tilde{g}$)-m($\tilde{\chi}_1^0$)=300 GeV | 1909.08457
3rd gen. squarks direct production
$\tilde{b}_1\tilde{b}_1$ | 0 e,μ | 2 b | E_T^{miss} | 139 | $\tilde{b}_1$ 1.255 | m($\tilde{\chi}_1^0$)<400 GeV | 2101.12527
$\tilde{b}_1$ 0.68 | 10 GeV<Δm($\tilde{b}_1$,$\tilde{\chi}_1^0$)<20 GeV | 2101.12527
$\tilde{b}_1\tilde{b}_1$, $\tilde{b}_1\to b\tilde{\chi}_2^0\to bh\tilde{\chi}_1^0$ | 0 e,μ | 6 b | E_T^{miss} | 139 | $\tilde{b}_1$ Forbidden 0.23-1.35 | Δm($\tilde{\chi}_2^0$,$\tilde{\chi}_1^0$)=130 GeV, m($\tilde{\chi}_1^0$)=100 GeV | 1908.03122
2 τ | 2 b | E_T^{miss} | 139 | $\tilde{b}_1$ 0.13-0.85 | Δm($\tilde{\chi}_2^0$,$\tilde{\chi}_1^0$)=130 GeV, m($\tilde{\chi}_1^0$)=0 GeV | ATLAS-CONF-2020-031
$\tilde{t}_1\tilde{t}_1$, $\tilde{t}_1\to t\tilde{\chi}_1^0$ | 0-1 e,μ | $\geq$ 1 jet | E_T^{miss} | 139 | $\tilde{t}_1$ 1.25 | m($\tilde{\chi}_1^0$)=1 GeV | 2004.14060, 2012.03799
$\tilde{t}_1\tilde{t}_1$, $\tilde{t}_1\to Wb\tilde{\chi}_1^0$ | 1 e,μ | 3 jets/1 b | E_T^{miss} | 139 | $\tilde{t}_1$ Forbidden 0.65 | m($\tilde{\chi}_1^0$)=500 GeV | 2012.03799
$\tilde{t}_1\tilde{t}_1$, $\tilde{t}_1\to\tilde{\tau}_1 b\nu$, $\tilde{\tau}_1\to\tau\tilde{G}$ | 1-2 τ | 2 jets/1 b | E_T^{miss} | 139 | $\tilde{t}_1$ Forbidden 1.4 | m($\tilde{\tau}_1$)=800 GeV | ATLAS-CONF-2021-008
$\tilde{t}_1\tilde{t}_1$, $\tilde{t}_1\to c\tilde{\chi}_1^0$ / $\tilde{c}\tilde{c}$, $\tilde{c}\to c\tilde{\chi}_1^0$ | 0 e,μ | 2 c | E_T^{miss} | 36.1 | $\tilde{c}$ 0.85 | m($\tilde{\chi}_1^0$)=0 GeV | 1805.01649
0 e,μ | mono-jet | E_T^{miss} | 139 | $\tilde{t}_1$ 0.55 | m($\tilde{t}_1$,$\tilde{c}$)-m($\tilde{\chi}_1^0$)=5 GeV | 2102.10874
$\tilde{t}_1\tilde{t}_1$, $\tilde{t}_1\to t\tilde{\chi}_2^0$, $\tilde{\chi}_2^0\to Z/h\tilde{\chi}_1^0$ | 1-2 e,μ | 1-4 b | E_T^{miss} | 139 | $\tilde{t}_1$ 0.067-1.18 | m($\tilde{\chi}_2^0$)=500 GeV | 2006.05880
$\tilde{t}_2\tilde{t}_2$, $\tilde{t}_2\to\tilde{t}_1 + Z$ | 3 e,μ | 1 b | E_T^{miss} | 139 | $\tilde{t}_2$ Forbidden 0.86 | m($\tilde{\chi}_1^0$)=360 GeV, m($\tilde{t}_1$)-m($\tilde{\chi}_1^0$)= 40 GeV | 2006.05880
EW direct
$\tilde{\chi}_1^\pm\tilde{\chi}_2^0$ via WZ | 3 e,μ | E_T^{miss} | 139 | $\tilde{\chi}_1^\pm/\tilde{\chi}_2^0$ 0.64 | m($\tilde{\chi}_1^0$)=0 | ATLAS-CONF-2020-015
$ee,\mu\mu$ | $\geq$ 1 jet | E_T^{miss} | 139 | $\tilde{\chi}_1^\pm/\tilde{\chi}_2^0$ 0.205 | m($\tilde{\chi}_1^\pm$)-m($\tilde{\chi}_1^0$)=5 GeV | 1911.12606
$\tilde{\chi}_1^\pm\tilde{\chi}_1^\mp$ via WW | 2 e,μ | E_T^{miss} | 139 | $\tilde{\chi}_1^\pm$ 0.42 | m($\tilde{\chi}_1^0$)=0 | 1908.08215
$\tilde{\chi}_1^\pm\tilde{\chi}_2^0$ via Wh | 0-1 e,μ | 2 b/2 γ | E_T^{miss} | 139 | $\tilde{\chi}_1^\pm/\tilde{\chi}_2^0$ Forbidden 0.74 | m($\tilde{\chi}_1^0$)=70 GeV | 2004.10894, 1909.09226
$\tilde{\chi}_1^\pm\tilde{\chi}_1^\mp$ via $\tilde{\ell}_L/\tilde{\nu}$ | 2 e,μ | E_T^{miss} | 139 | $\tilde{\chi}_1^\pm$ 1.0 | m($\tilde{\ell}$,$\tilde{\nu}$)=0.5(m($\tilde{\chi}_1^\pm$)+m($\tilde{\chi}_1^0$)) | 1908.08215
$\tilde{\tau}\tilde{\tau}$, $\tilde{\tau}\to\tau\tilde{\chi}_1^0$ | 2 τ | E_T^{miss} | 139 | $\tilde{\tau}$ [$\tilde{\tau}_L$, $\tilde{\tau}_{R,L}$] 0.16-0.3 0.12-0.39 | m($\tilde{\chi}_1^0$)=0 | 1911.06660
$\tilde{\ell}_{L,R}\tilde{\ell}_{L,R}$, $\tilde{\ell}\to\ell\tilde{\chi}_1^0$ | 2 e,μ | 0 jets | E_T^{miss} | 139 | $\tilde{\ell}$ 0.7 | m($\tilde{\chi}_1^0$)=0 | 1908.08215
$ee,\mu\mu$ | $\geq$ 1 jet | E_T^{miss} | 139 | $\tilde{\ell}$ 0.256 | m($\tilde{\ell}$)-m($\tilde{\chi}_1^0$)=10 GeV | 1911.12606
$\tilde{H}\tilde{H}$, $\tilde{H}\to h\tilde{G}/Z\tilde{G}$ | 0 e,μ | $\geq$ 3 b | E_T^{miss} | 36.1 | $\tilde{H}$ 0.13-0.23 0.29-0.88 | BR($\tilde{\chi}_1^0\to h\tilde{G}$)=1 | 1806.04030
4 e,μ | 0 jets | E_T^{miss} | 139 | $\tilde{H}$ 0.55 | BR($\tilde{\chi}_1^0\to Z\tilde{G}$)=1 | 2103.11684
Long-lived particles
Direct $\tilde{\chi}_1^+\tilde{\chi}_1^-$ prod., long-lived $\tilde{\chi}_1^\pm$ | Disapp. trk | 1 jet | E_T^{miss} | 139 | $\tilde{\chi}_1^\pm$ 0.66 | Pure Wino | ATLAS-CONF-2021-015
$\tilde{\chi}_1^\pm$ 0.21 | Pure higgsino | ATLAS-CONF-2021-015
Stable $\tilde{g}$ R-hadron | Multiple | 36.1 | $\tilde{g}$ 2.0 | 1902.01636, 1808.04095
Metastable $\tilde{g}$ R-hadron, $\tilde{g}\to qq\tilde{\chi}_1^0$ | Multiple | 36.1 | $\tilde{g}$ [$\tau(\tilde{g})$ =10 ns, 0.2 ns] 2.05 2.4 | m($\tilde{\chi}_1^0$)=100 GeV | 1710.04901, 1808.04095
$\tilde{\ell}\tilde{\ell}$, $\tilde{\ell}\to\ell\tilde{G}$ | Displ. lep | E_T^{miss} | 139 | $\tilde{e}$,$\tilde{\mu}$ 0.7 | $\tau(\tilde{\ell})$ = 0.1 ns | 2011.07812
$\tilde{\tau}$ 0.34 | $\tau(\tilde{\ell})$ = 0.1 ns | 2011.07812
RPV
$\tilde{\chi}_1^\pm\tilde{\chi}_1^\mp/\tilde{\chi}_1^0$, $\tilde{\chi}_1^\pm\to Z\ell\to\ell\ell\ell$ | 3 e,μ | 139 | $\tilde{\chi}_1^\pm/\tilde{\chi}_1^0$ [BR($Z\tau$)=1, BR(Ze)=1] 0.625 1.05 | Pure Wino | 2011.10543
$\tilde{\chi}_1^\pm\tilde{\chi}_1^\mp/\tilde{\chi}_2^0\to WW/Z\ell\ell\ell\ell\nu\nu$ | 4 e,μ | 0 jets | E_T^{miss} | 139 | $\tilde{\chi}_1^\pm/\tilde{\chi}_2^0$ [$\lambda_{133}\neq 0$, $\lambda_{12k}\neq 0$] 0.95 1.55 | m($\tilde{\chi}_1^0$)=200 GeV | 2103.11684
$\tilde{g}\tilde{g}$, $\tilde{g}\to qq\tilde{\chi}_1^0$, $\tilde{\chi}_1^0\to qqq$ | 4-5 large-R jets | 36.1 | $\tilde{g}$ [m($\tilde{\chi}_1^0$)=200 GeV, 1100 GeV] 1.3 1.9 | Large λ''_{112} | 1804.03568
$\tilde{t}\tilde{t}$, $\tilde{t}\to t\tilde{\chi}_1^0$, $\tilde{\chi}_1^0\to tbs$ | Multiple | 36.1 | $\tilde{t}$ [λ''_{323}=2e-4, 1e-2] 0.55 1.05 | m($\tilde{\chi}_1^0$)=200 GeV, bino-like | ATLAS-CONF-2018-003
$\tilde{t}\tilde{t}$, $\tilde{t}\to b\tilde{\chi}_1^\pm$, $\tilde{\chi}_1^\pm\to bbs$ | $\geq$ 4b | 139 | $\tilde{t}$ Forbidden 0.95 | m($\tilde{\chi}_1^\pm$)=500 GeV | 2010.01015
$\tilde{t}_1\tilde{t}_1$, $\tilde{t}_1\to bs$ | 2 jets + 2 b | 36.7 | $\tilde{t}_1$ [qq, $b\ell$] 0.42 0.61 | 1710.07171
$\tilde{t}_1\tilde{t}_1$, $\tilde{t}_1\to q\ell$ | 2 e,μ | 2 b | 36.1 | $\tilde{t}_1$ 0.4-1.45 | BR($\tilde{t}_1\to be/b\mu$)>20% | 1710.05544
1 μ | DV | 136 | $\tilde{t}_1$ [1e-10< λ'_{23k} <1e-8, 3e-10< λ'_{23k} <3e-9] 1.0 1.6 | BR($\tilde{t}_1\to q\mu$)=100%, cosθ_t=1 | 2003.11956
$\tilde{\chi}_1^\pm/\tilde{\chi}_2^0/\tilde{\chi}_1^0$, $\tilde{\chi}_{1,2}^0\to tbs$, $\tilde{\chi}_1^+\to bbs$ | 1-2 e,μ | $\geq$6 jets | 139 | $\tilde{\chi}_1^0$ 0.2-0.32 | Pure higgsino | ATLAS-CONF-2021-007
10^{-1}
1
Mass scale [TeV]
*Only a selection of the available mass limits on new states or phenomena is shown. Many of the limits are based on simplified models, c.f. refs. for the assumptions made.

Conclusion

- Presented four of the most recent ATLAS SUSY analyses
- These analyses cover a large range of models and SUSY parameters
- Improvements in background estimation techniques and even custom datasets are used to improve analyses
- Delivered excellent exclusion limits for a number of models

To the future

- Many more results to come in this sphere on processes and final states not discussed here
- Significant advancements in analysis techniques promise even better results in the future
- Combination efforts are underway to harmonise the results of a range of analyses
- For a complete list of ATLAS SUSY results check out: ATLAS Public Results
- More BSM talks at DIS: leptoquarks, dark matter, Higgs-like resonances, Higgs+DM.

Thanks for your attention!

Disappearing track candidate with $p_{\mathrm{T}} = 1.2$ TeV

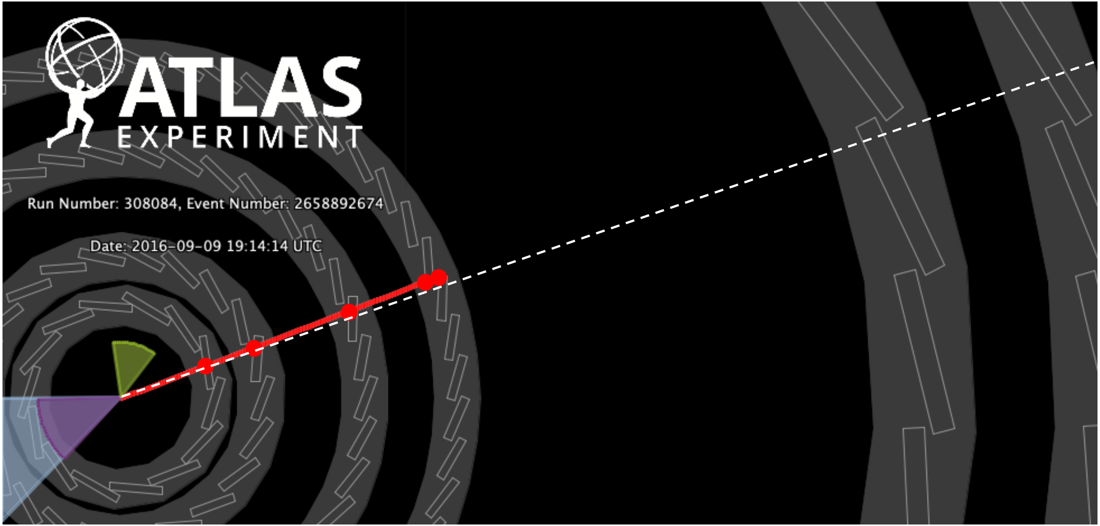

Stop to stau additional material

MC samples

Physics process	Generator	Parton shower	Tune	Cross section	PDF (generator)	PDF (PS)
$t\bar{t}$	Powheg-Box v2	Pythia 8.230	A14	NNLO+NNLL	NNPDF3.0NLO	NNPDF2.3LO
Single top	Powheg-Box v2	Pythia 8.230	A14	NLO+NNLL	NNPDF3.0NLO	NNPDF2.3LO
$\mathrm{V} + jets(V = W, Z)$	Sherpa 2.2.1	Sherpa 2.2.1	Sherpa default	NNLO	NNPDF3.0NNLO	NNPDF3.0NNLO
Diboson VV $(V = W, Z)$	Sherpa 2.2.1 or 2.2.2	Sherpa 2.2.1 or 2.2.2	Sherpa default	NLO	NNPDF3.0NNLO	NNPDF3.0NNLO
Triboson VVV $(V = W, Z)$	Sherpa 2.2.1	Sherpa 2.2.1	Sherpa default	NLO	NNPDF3.0NNLO	NNPDF3.0NNLO
$t\bar{t} + V(V = W, Z)$	MadGraph5_aMC@NLO 2.3.3	Pythia 8.210	A14	NLO	NNPDF3.0NLO	NNPDF2.3LO
$t\bar{t} + H$	Powheg-Box v2	Pythia 8.230	A14	NLO	NNPDF3.0NLO	NNPDF2.3LO
$t\bar{t} + WW$	MadGraph5_aMC@NLO 2.2.2	Pythia 8.186	A14	NLO	NNPDF2.3LO	NNPDF2.3LO
$t\bar{t} + WZ$	MadGraph5_aMC@NLO 2.3.3	Pythia 8.212	A14	NLO	NNPDF3.0NLO	NNPDF2.3LO
tWZ	MadGraph5_aMC@NLO 2.3.3	Pythia 8.212	A14	NLO	NNPDF3.0NLO	NNPDF2.3LO
$tZ, t\bar{t}t, t\bar{t}t\bar{t}$	MadGraph5_aMC@NLO 2.3.3	Pythia 8.230	A14	NLO	NNPDF3.1NLO	NNPDF2.3LO
Stop-stau	MadGraph5_aMC@NLO 2.6.2	Pythia 8.212	A14	approx. NNLO+NNLL	NNPDF2.3LO	NNPDF2.3LO
$\mathrm{LQ}_3^{\mathrm{u/d}}$	MadGraph5_aMC@NLO 2.6.0	Pythia 8.230	A14	approx. NNLO+NNLL	NNPDF3.0NLO	NNPDF2.3LO

Preselection

Di-tau preselection	Single-tau preselection
$E_{\mathrm{T}}^{\mathrm{miss}}$-trigger fired and $E_{\mathrm{T}}^{\mathrm{miss}} > 250\,\mathrm{GeV}$	
No light leptons (e/μ)	
At least two jets	
At least one b-tagged jet	
At least two hadronic tau candidates	Exactly one hadronic tau candidate
	At least two b-tagged jets

Signal regions

Variable	CR $t\bar{t}$ (2 real τ)	CR $t\bar{t}$ (1 real τ)	VR $t\bar{t}$ (2 real τ)	VR $t\bar{t}$ (1 real τ)	SR
$E_{\mathrm{T}}^{\mathrm{miss}}$	—	—	—	—	> 280 GeV
$OS(\tau_1, \tau_2)$	1	—	1	—	1
$m_{\mathrm{T2}}(\tau_1, \tau_2)$	< 35 GeV	< 35 GeV	$[35, 70]$ GeV	$[35, 70]$ GeV	> 70 GeV
$m(\tau_1, \tau_2)$	> 50 GeV	> 50 GeV	—	—	—
$m_{\mathrm{T}}(\tau_1)$	> 50 GeV	< 50 GeV	> 70 GeV	< 70 GeV	—

Variable	CR $t\bar{t}$ (1 real τ)	CR single top	VR $t\bar{t}$ (1 real τ)	VR single top	SR
$E_{\mathrm{T}}^{\mathrm{miss}}$	> 280 GeV	> 280 GeV	> 280 GeV	> 280 GeV	> 280 GeV
s_{T}	$[500, 600]$ GeV	—	> 600 GeV	—	$> 800(600)$ GeV
$\sum m_{\mathrm{T}}(b_{1,2})$	$[600, 700]$ GeV	> 800 GeV	$[600, 700]$ GeV	> 800 GeV	> 700 GeV
$m_{\mathrm{T}}(\tau)$	—	< 50 GeV	—	$[50, 150]$ GeV	$> 300(150)$ GeV
$p_{\mathrm{T}}(\tau)$	—	> 80 GeV	—	> 80 GeV	— (binned)

Uncertainties

Systematic uncertainty	Di-tau SR	Single-tau one-bin SR	Single-tau multi-bin SR
Total	25 %	17 %	17 %
Jet-related	19 %	4.2 %	3.9 %
Tau-related	4.7 %	5.5 %	4.3 %
Other experimental	3.7 %	1.0 %	0.8 %
Theoretical modelling	13 %	17 %	19 %
MC statistics	12 %	7.5 %	4.4 %
Normalisation factors	8.8 %	15 %	16 %
Luminosity	0.8 %	0.5 %	0.4 %

SR table

	Di-tau SR	Single-tau SR (one-bin)	Single-tau SR (binned in $p_{\mathrm{T}}(\tau)$)		
			[50, 100] GeV	[100, 200] GeV	$>$ 200 GeV
Observed	2	6	8	6	2
Total bkg.	4.1 ± 1.0	3.23 ± 0.55	10.1 ± 1.8	5.1 ± 1.1	2.05 ± 0.64
$t\bar{t}$ (2 real τ)	0.81 ± 0.71	—	—	—	—
$t\bar{t}$ (1 real τ)	0.82 ± 0.27	1.20 ± 0.30	4.8 ± 1.2	2.69 ± 0.88	0.64 ± 0.29
$t\bar{t}$-fake	0.51 ± 0.15	0.69 ± 0.15	2.83 ± 0.87	0.66 ± 0.17	0.185 ± 0.072
Single top	0.03 $\pm^{0.10}_{0.03}$	0.39 $\pm^{0.45}_{0.39}$	0.85 $\pm^{0.86}_{0.85}$	0.54 ± 0.54	0.57 ± 0.56
$W+$jets	0.08 $\pm^{0.11}_{0.08}$	0.35 ± 0.16	0.34 ± 0.12	0.64 ± 0.24	0.37 ± 0.12
$Z+$jets	0.35 ± 0.14	0.187 ± 0.054	0.275 ± 0.081	0.043 ± 0.022	0.123 ± 0.048
Multiboson	0.48 ± 0.21	0.085 ± 0.037	0.163 ± 0.037	0.111 ± 0.030	0.030 $\pm^{0.032}_{0.030}$
$t\bar{t}+V$	0.60 ± 0.15	0.242 ± 0.064	0.65 ± 0.16	0.31 ± 0.12	0.092 ± 0.035
$t\bar{t}+H$	0.28 $\pm^{0.29}_{0.28}$	0.039 $\pm^{0.040}_{0.039}$	0.10 ± 0.10	0.060 $\pm^{0.061}_{0.060}$	0.028 $\pm^{0.029}_{0.028}$
Other top	0.122 ± 0.067	0.043 ± 0.022	0.096 ± 0.074	0.091 ± 0.049	0.0120 ± 0.0084

Model independent upper limits

Signal channel	$\langle A\epsilon\sigma\rangle^{95}_{\rm obs}$ [fb]	$S^{95}_{\rm obs}$	$S^{95}_{\rm exp}$	CL_b	$p(s=0)$ (Z)
Di-tau SR	0.03	4.1	$5.3^{+2.2}_{-1.5}$	0.18	0.50 (0.0)
Single-tau one-bin SR	0.06	8.2	$5.1^{+2.1}_{-1.3}$	0.91	0.08 (1.37)

RPV additional material

Branching ratios

LSP type	Branching ratios for sparticle: stop		gluino			Cross-section [fb] for direct production		
	t	$b\tilde{\chi}_1^\pm$	tt	bb	$tb\tilde{\chi}_1^\pm$	$\tilde{\chi}_1^\pm\tilde{\chi}_1^0$	$\tilde{\chi}_1^\pm\tilde{\chi}_2^0$	$\tilde{\chi}_2^0\tilde{\chi}_1^0$
Bino	100%	0%	100%	0%	0%	0	0	0
Wino	33%	66%	16%	16%	66%	387	0	0
Higgsino	50%	50%	50%	0%	50%	91	91	52

MC samples

Physics process	Event generator	Parton-shower modelling	Cross-section normalisation	PDF set	Tune
$W(\to \ell\nu)$ + jets	Sherpa 2.2.1 [66]	Sherpa 2.2.1	NNLO [67]	NNPDF3.0nnlo [68]	Sherpa
$W(\to \ell\nu)$ + jets (*)	MG5_aMC 2.2.2 [47]	Pythia 8.186 [69]	NNLO	NNPDF3.0nlo [68]	A14 [70]
$Z/\gamma^*(\to \ell\ell)$ + jets	Sherpa 2.2.1	Sherpa 2.2.1	NNLO [67]	NNPDF3.0nnlo	Sherpa
$t\bar{t}$ + jets	PowhegBox v2 [71,72,73,74]	Pythia 8.230 [43]	NNLO+NNLL [75,76,77,78,79,80,81]	NNPDF3.0nlo	A14
$t\bar{t}$ + jets (*)	PowhegBox v2	Herwig7.04 [82,83]	NNLO+NNLL	MMHT2014lo [84]	H7UE [83]
$t\bar{t}$ + jets (*)	MG5_aMC 2.6.0	Pythia 8.230	NNLO+NNLL	NNPDF3.0nlo	A14
Single-top	PowhegBox v2 [85,86,87]	Pythia 8.230	NNLO+NNLL [88,89,90]	NNPDF3.0nlo	A14
$t\bar{t} + W/Z$	Sherpa 2.2.1	Sherpa 2.2.1	NLO [91]	NNPDF3.0nnlo	Sherpa
$t\bar{t} + t\bar{t}/t/WW/WZ$	MG5_aMC 2.3.3 [47]	Pythia 8.230	NLO [91] ($t\bar{t}t$ LO)	NNPDF2.3lo [44]	A14
$t\bar{t}t\bar{t}$ (*)	MG5_aMC 2.3.3	Herwig7.04	NLO [47]	MMHT2014lo	H7UE
$t\bar{t}H$	PowhegBox v2	Pythia 8.230	NLO	NNPDF3.0nlo	A14
tWZ, tZ	MG5_aMC 2.3.3	Pythia 8.212, 8.210	NLO	NNPDF3.0nlo	A14
VV and VVV	Sherpa 2.2.1, 2.2.2, 2.2.4	Sherpa	NLO	NNPDF3.0nnlo	Sherpa

Jet ratios

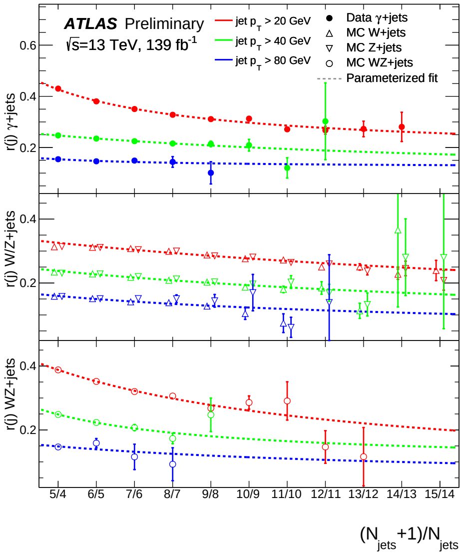

ATLAS Preliminary
√s=13 TeV, 139 fb-1
jet pT > 20 GeV
jet pT > 40 GeV
jet pT > 80 GeV
Data γ+jets
MC W+jets
MC Z+jets
MC WZ+jets
Parameterized fit
r(j) γ+jets
r(j) W/Z+jets
r(j) WZ+jets
(Njets+1)/Njets

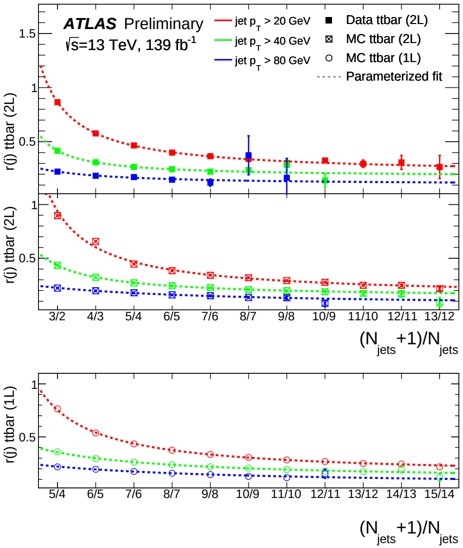

ATLAS Preliminary
√s=13 TeV, 139 fb-1
jet pT > 20 GeV
jet pT > 40 GeV
jet pT > 80 GeV
Data ttbar (2L)
MC ttbar (2L)
MC ttbar (1L)
Parameterized fit
r(j) ttbar (2L)
r(j) ttbar (1L)
(Njets+1)/Njets

Background estimation

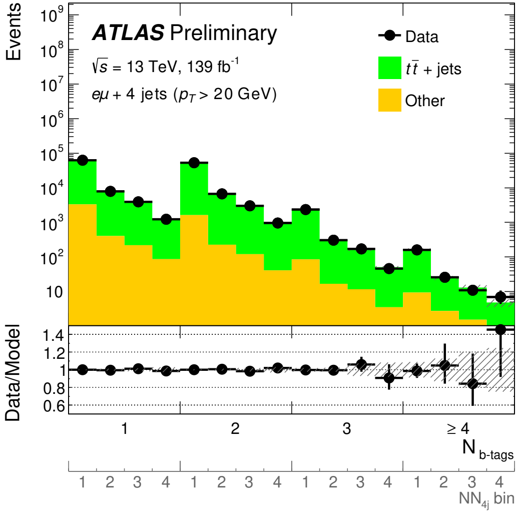

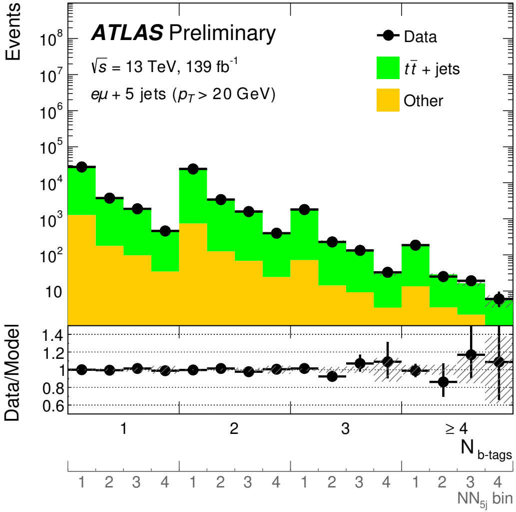

Floating parameters

Parameters	$t\bar{t}$ +jets	$t\bar{t}X^{\text{sc}}$	W+jets	Z+jets	VV+jets	Constraints
Normalization	$N_4^{t\bar{t}}$	$N_4^{t\bar{t}X^{\text{sc}}}$	N_4^W	N_4^Z	N_4^{VV}	–
Jet scaling, $i \in \{0,1,2\}$	$c_i^{t\bar{t}}$	$c_i^{t\bar{t}X^{\text{sc}}}$	$c_i^{W/Z}$		c_i^{VV}	$c_2^{W/Z} = c_2^{VV} = 1$
Initial b-jet fractions, $i \in \{0 \ldots 4\}$	$f_{4,i}^{t\bar{t}}$	$f_{4,i}^{t\bar{t}X^{\text{sc}}}$	–	–	–	$\sum_i f_{4,i} = 1$
Extra heavy-flavour jets, $i \in \{0,1,2\}$	$x_i,\ \rho_{11}$		–	–	–	$\sum_i x_i = 1$
NN shape, $i \in \{1 \ldots 4\}$, $j \in \{4 \ldots 8\}$	$n_{j,i}$	–	–	–	–	$\sum_i n_{j,i} = 1$

Pulls

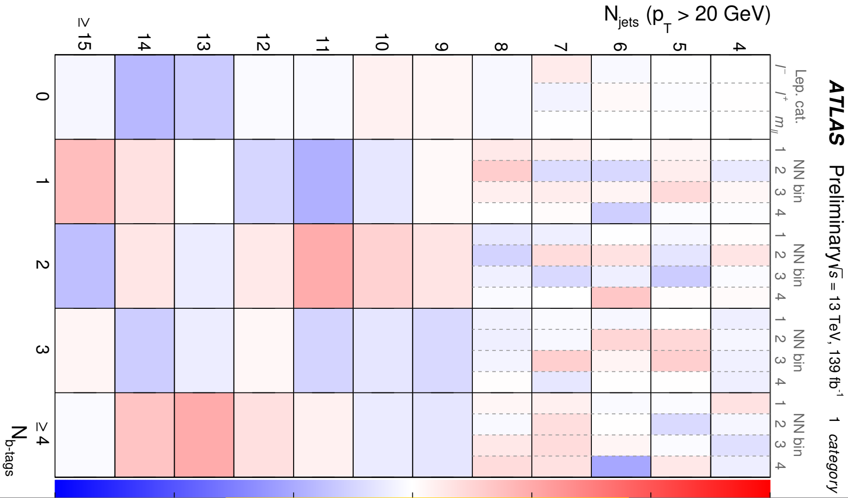
ATLAS Preliminary $\sqrt{s}$ = 13 TeV, 139 fb^{-1}
1 category
N_{jets} (p_T > 20 GeV)
$N_{b\text{-tags}}$
Lep. cat.
NN bin

Pulls 2

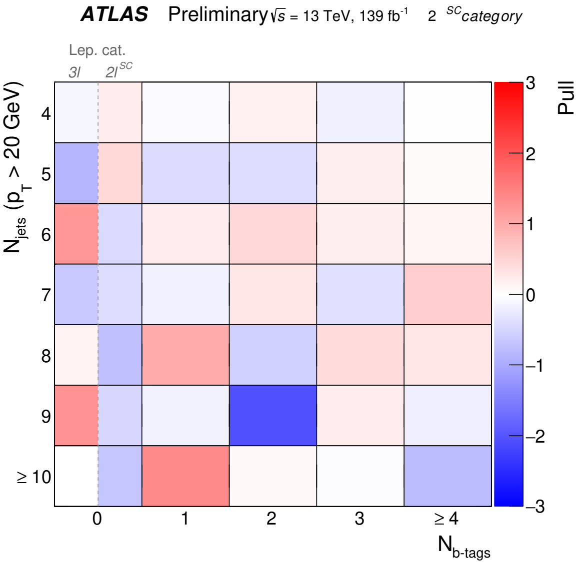
ATLAS Preliminary $\sqrt{s}$ = 13 TeV, 139 fb^{-1} 2 ^{SC}category
Lep. cat.
3l 2l^{SC}
N_{jets} (p_T > 20 GeV)
4
5
6
7
8
9
≥ 10
0
1
2
3
≥ 4
$N_{b\text{-}tags}$
Pull
3
2
1
0
−1
−2
−3

Model independent results

Jet p_T threshold	Selection †=NN bin 4	Total background	Data	p_0	Z	σ^{excl} obs. [ab]	σ^{excl} exp. [ab]
20 GeV	$= 6j, \geq 4b$,†	145 ± 6	126	0.5	0	130	200^{+80}_{-60}
	$\geq 15j, = 0b$	16.3 ± 3.3	16	0.5	0	100	100^{+40}_{-30}
	$\geq 15j, \geq 3b$	17.0 ± 1.9	20	0.26	0.7	92	74^{+29}_{-21}
40 GeV	$\geq 12j, = 0b$	7.8 ± 1.5	8	0.47	0.1	55	53^{+21}_{-15}
	$\geq 12j, \geq 3b$	8.6 ± 1.1	12	0.17	0.9	76	55^{+21}_{-15}
60 GeV	$\geq 11j, = 0b$	2.7 ± 0.8	3	0.44	0.2	38	35^{+14}_{-10}
	$\geq 11j, \geq 3b$	2.3 ± 0.6	5	0.1	1.3	56	33^{+13}_{-9}
80 GeV	$\geq 10j, = 0b$	2.1 ± 1.1	3	0.38	0.3	42	34^{+13}_{-9}
	$\geq 10j, \geq 3b$	1.7 ± 1.5	2	0.47	0.1	35	33^{+13}_{-9}
100 GeV	$\geq 8j, = 0b$	22.7 ± 1.9	25	0.38	0.3	96	85^{+33}_{-24}
	$\geq 8j, \geq 3b$	7.5 ± 1.0	8	0.41	0.2	55	51^{+20}_{-14}

Jet p_T threshold	Selection †=$m^{\ell j} < 155$ GeV	Total background	Data	p_0	Z	σ^{excl} obs. [ab]	σ^{excl} exp. [ab]
20 GeV	$= 6j, \geq 3b$,†	16.1 ± 1.2	20	0.21	0.8	92	69^{+27}_{-19}
	$\geq 10j, = 0b$	5.8 ± 0.8	6	0.46	0.1	48	45^{+18}_{-13}
	$\geq 10j, \geq 3b$	8.2 ± 1.5	6	0.5	0	41	54^{+21}_{-15}
40 GeV	$\geq 8j, = 0b$	2.8 ± 0.7	2	0.5	0	31	35^{+14}_{-10}
	$\geq 8j, \geq 3b$	3.6 ± 1.2	7	0.13	1.1	67	39^{+15}_{-11}
60 GeV	$\geq 7j, = 0b$	1.71 ± 0.35	3	0.2	0.8	41	29^{+12}_{-8}
	$\geq 7j, \geq 3b$	2.0 ± 0.7	5	0.09	1.3	58	32^{+13}_{-9}
80 GeV	$\geq 7j, = 0b$	0.34 ± 0.13	0	0.5	0	22	22^{+9}_{-0}
	$\geq 7j, \geq 3b$	0.54 ± 0.20	1	0.34	0.4	27	22^{+9}_{-0}
100 GeV	$\geq 6j, = 0b$	0.5 ± 0.4	0	0.5	0	22	22^{+9}_{-0}
	$\geq 6j, \geq 3b$	0.52 ± 0.22	1	0.28	0.6	28	22^{+9}_{-0}

Disappearing track additional material

Calorimeter energy

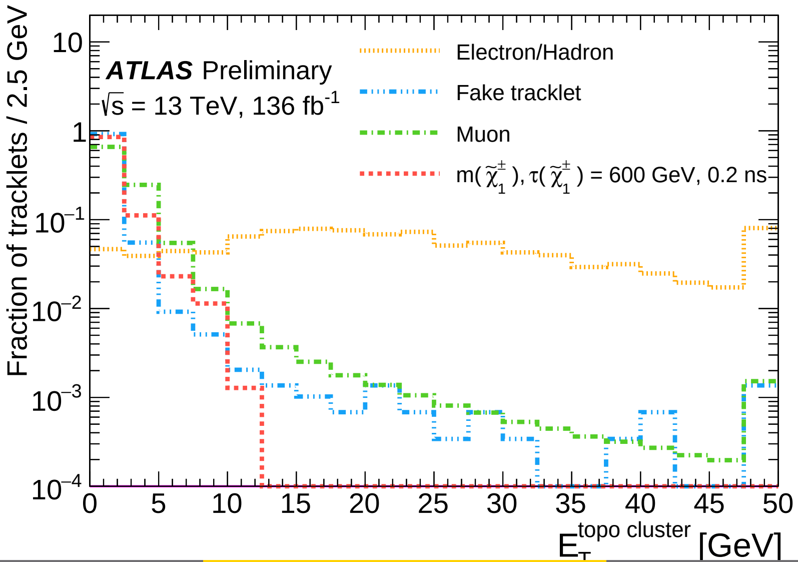

Signal region

Signal region	Electroweak production	Strong production
Number of electrons and muons	0	
Number of pixel tracklets	≥ 1	
$E_{\mathrm{T}}^{\mathrm{miss}}$ [GeV]	> 200	> 250
Number of jets ($p_{\mathrm{T}} > 20$ GeV)	≥ 1	≥ 3
Leading jet p_{T} [GeV]	> 100	> 100
Second and third jet p_{T} [GeV]	–	> 20
$\Delta\phi_{min}^{\mathrm{jet}-E_{\mathrm{T}}^{\mathrm{miss}}}$	> 1.0	> 0.4

Signal region expectation

Signal production channel	Electroweak production		Strong production	
$\tau_{\tilde{\chi}_1^\pm}$	0.2 ns	1.0 ns	0.2 ns	1.0 ns
$E_{\mathrm{T}}^{\mathrm{miss}}$ trigger	770.8 ± 6.8	775.3 ± 5.2	3177 ± 22	3177 ± 22
Lepton veto	769.4 ± 6.8	774.2 ± 5.2	3165 ± 22	3165 ± 22
$E_{\mathrm{T}}^{\mathrm{miss}} > 200$ GeV	394.5 ± 5.2	390.9 ± 4.0	–	–
$E_{\mathrm{T}}^{\mathrm{miss}} > 250$ GeV	–	–	1852 ± 17	1852 ± 17
Leading jet $p_{\mathrm{T}} > 100$ GeV	389.7 ± 5.2	384.9 ± 4.0	1848 ± 17	1848 ± 17
Third jet $p_{\mathrm{T}} > 20$ GeV	–	–	1834 ± 17	1834 ± 17
$\Delta\phi_{\mathrm{min}}^{\mathrm{jet}-\mathrm{E}_{\mathrm{T}}^{\mathrm{miss}}} > 0.4$	366.7 ± 5.0	362.3 ± 3.9	–	–
$\Delta\phi_{\mathrm{min}}^{\mathrm{jet}-\mathrm{E}_{\mathrm{T}}^{\mathrm{miss}}} > 1.0$	–	–	1578 ± 16	1578 ± 16
Pixel tracklet selection ($p_{\mathrm{T}} > 60$ GeV)	8.6 ± 0.6	27.3 ± 0.8	16.0 ± 1.3	105.0 ± 3.3

Control and validation regions

Region	$E_{\mathrm{T}}^{\mathrm{miss}}$ condition	Track condition
	Control regions	
Electron	e-subtracted $E_{\mathrm{T}}^{\mathrm{miss}}$	well-identified electron
Muon	μ-subtracted $E_{\mathrm{T}}^{\mathrm{miss}}$	well-identified muon
Hadron	standard $E_{\mathrm{T}}^{\mathrm{miss}}$	inner detector track
Fake-tracklet	standard $E_{\mathrm{T}}^{\mathrm{miss}}$	pixel-tracklet with $\|d_0/\sigma_{d_0}\| > 10$
	Low-$E_{\mathrm{T}}^{\mathrm{miss}}$ control region	
Low-$E_{\mathrm{T}}^{\mathrm{miss}}$	standard $E_{\mathrm{T}}^{\mathrm{miss}}$	pixel-tracklet
	Middle-$E_{\mathrm{T}}^{\mathrm{miss}}$ validation regions	
Low p_{T}	standard $E_{\mathrm{T}}^{\mathrm{miss}}$	pixel-tracklet with $p_{\mathrm{T}} < 60$ GeV
Calorimeter side-band	standard $E_{\mathrm{T}}^{\mathrm{miss}}$	pixel-tracklet with 5 GeV$< E_{\mathrm{T}}^{\mathrm{clus}} < 10$ GeV

Smearing parameters

	Muon		Electron	
Transverse momentum	σ [TeV^{-1}]	α	σ [TeV^{-1}]	α
$10 < p_{\mathrm{T}} < 15$	16.96	1.72	20.94	1.86
$15 < p_{\mathrm{T}} < 20$	15.54	1.72	19.54	1.86
$15 < p_{\mathrm{T}} < 25$	14.91	1.72	18.33	1.86
$25 < p_{\mathrm{T}} < 35$	14.84	1.72	17.01	1.86
$35 < p_{\mathrm{T}} < 45$	14.21	1.66	15.42	1.82
$45 < p_{\mathrm{T}} < 60$	13.64	1.62	14.49	1.66
$60 < p_{\mathrm{T}} < 100$	13.44	1.68	13.90	1.54
$100 < p_{\mathrm{T}}$	13.21	1.64	14.03	1.64

Systematics

	Electroweak channel [%]	Strong channel [%]
r_{ABCD}	5.2	0.9
r_{CD}	3.2	0.6
σ in signal p_{T} smearing function	2.9	0.1
α in signal p_{T} smearing function	1.7	0.2
p_0 parameter in the fake background p_{T} function	0.3	$<$0.1
p_1 parameter in the fake background p_{T} function	0.3	0.2
Normalization of muon background	0.6	$<$0.1
Normalization of electron background	$<$0.1	$<$0.1
α in muon p_{T} smearing function	$<$0.1	$<$0.1
σ in muon p_{T} smearing function	$<$0.1	$<$0.1
α in electron p_{T} smearing function	$<$0.1	$<$0.1
σ in electron p_{T} smearing function	$<$0.1	$<$0.1
α in hadron p_{T} smearing function	0.5	0.2
σ in hadron p_{T} smearing function	0.6	0.2

Signal uncertainty

	Electroweak channel [%] $m_{\tilde{\chi}_1^\pm} = 600$ GeV	Strong channel [%] $m_{\tilde{g}} = 1400$ GeV $m_{\tilde{\chi}_1^\pm} = 1100$ GeV
Cross-section	7.6	14
Initial/final state radiation	8.4	5.1
Jet energy scale	2.3	1.5
Jet energy resolution	0.6	0.3
Jet vertex tagging efficiency	<0.1	<0.1
Pile-up modelling	0.7	<0.1
$E_{\mathrm{T}}^{\mathrm{miss}}$ soft term	0.4	<0.1
Trigger efficiency	0.3	0.4
Tracklet reconstruction efficiency	5.9	5.9
Luminosity	1.7	1.7
Total	11	8.1

Electroweak fits

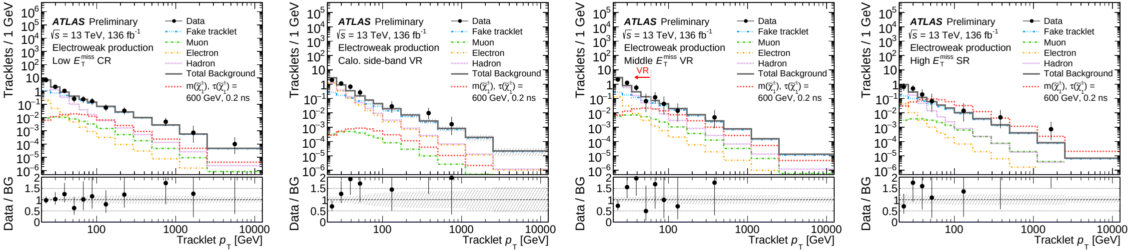

Strong fits

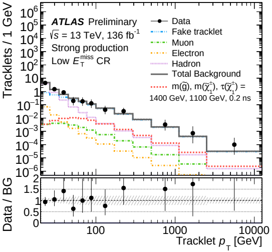
ATLAS Preliminary
√s = 13 TeV, 136 fb-1
Strong production
Low E_T^miss CR
Data
Fake tracklet
Muon
Electron
Hadron
Total Background
m(g̃), m(χ̃1±), τ(χ̃1±) =
1400 GeV, 1100 GeV, 0.2 ns
Tracklets / 1 GeV
Data / BG
Tracklet p_T [GeV]

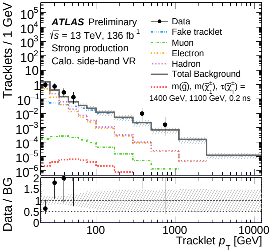
ATLAS Preliminary
√s = 13 TeV, 136 fb-1
Strong production
Calo. side-band VR
Data
Fake tracklet
Muon
Electron
Hadron
Total Background
m(g̃), m(χ̃1±), τ(χ̃1±) =
1400 GeV, 1100 GeV, 0.2 ns
Tracklets / 1 GeV
Data / BG
Tracklet p_T [GeV]

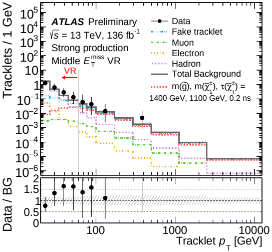
ATLAS Preliminary
√s = 13 TeV, 136 fb-1
Strong production
Middle E_T^miss VR
VR
Data
Fake tracklet
Muon
Electron
Hadron
Total Background
m(g̃), m(χ̃1±), τ(χ̃1±) =
1400 GeV, 1100 GeV, 0.2 ns
Tracklets / 1 GeV
Data / BG
Tracklet p_T [GeV]

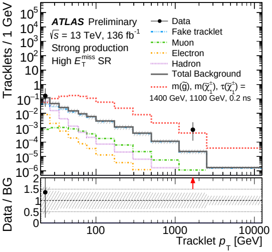
ATLAS Preliminary
√s = 13 TeV, 136 fb-1
Strong production
High E_T^miss SR
Data
Fake tracklet
Muon
Electron
Hadron
Total Background
m(g̃), m(χ̃1±), τ(χ̃1±) =
1400 GeV, 1100 GeV, 0.2 ns
Tracklets / 1 GeV
Data / BG
Tracklet p_T [GeV]

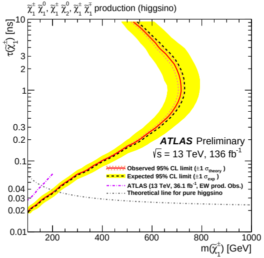
production (higgsino)
ATLAS Preliminary
√s = 13 TeV, 136 fb-1
Observed 95% CL limit (±1 σtheory)
Expected 95% CL limit (±1 σexp)
ATLAS (13 TeV, 36.1 fb-1, EW prod. Obs.)
Theoretical line for pure higgsino
m(χ̃1±) [GeV]
τ(χ̃1±) [ns]

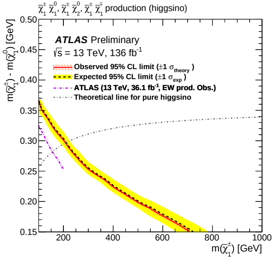
production (higgsino)
ATLAS Preliminary
√s = 13 TeV, 136 fb-1
Observed 95% CL limit (±1 σtheory)
Expected 95% CL limit (±1 σexp)
ATLAS (13 TeV, 36.1 fb-1, EW prod. Obs.)
Theoretical line for pure higgsino
m(χ̃1±) [GeV]
m(χ̃1±) - m(χ̃10) [GeV]

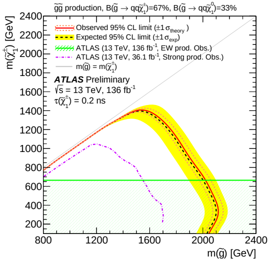
g̃g̃ production, B(g̃ → qqχ̃1±)=67%, B(g̃ → qqχ̃10)=33%
Observed 95% CL limit (±1 σtheory)
Expected 95% CL limit (±1 σexp)
ATLAS (13 TeV, 136 fb-1, EW prod. Obs.)
ATLAS (13 TeV, 36.1 fb-1, Strong prod. Obs.)
m(g̃) = m(χ̃1±)
ATLAS Preliminary
√s = 13 TeV, 136 fb-1
τ(χ̃1±) = 0.2 ns
m(g̃) [GeV]
m(χ̃1±) [GeV]

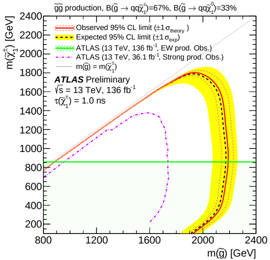
g̃g̃ production, B(g̃ → qqχ̃1±)=67%, B(g̃ → qqχ̃10)=33%
Observed 95% CL limit (±1 σtheory)
Expected 95% CL limit (±1 σexp)
ATLAS (13 TeV, 136 fb-1, EW prod. Obs.)
ATLAS (13 TeV, 36.1 fb-1, Strong prod. Obs.)
m(g̃) = m(χ̃1±)
ATLAS Preliminary
√s = 13 TeV, 136 fb-1
τ(χ̃1±) = 1.0 ns
m(g̃) [GeV]
m(χ̃1±) [GeV]

Event display 1

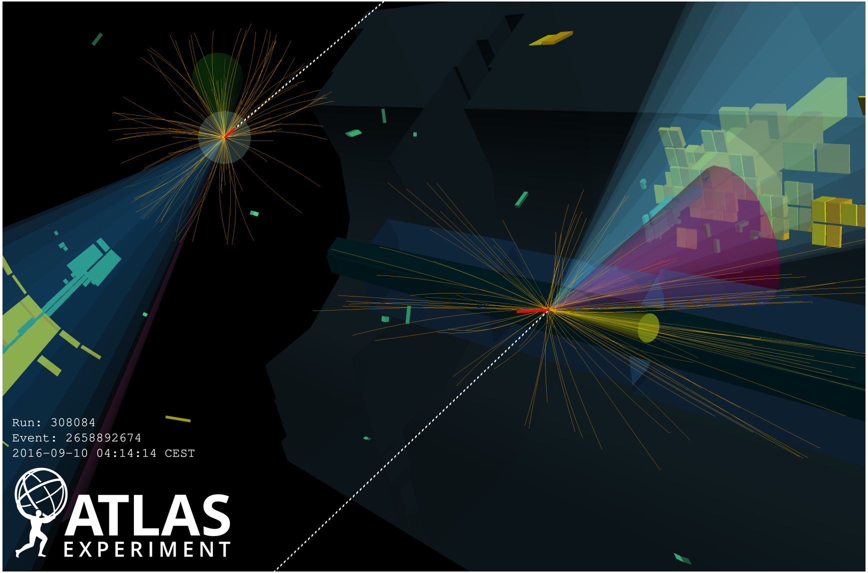

Event display 2

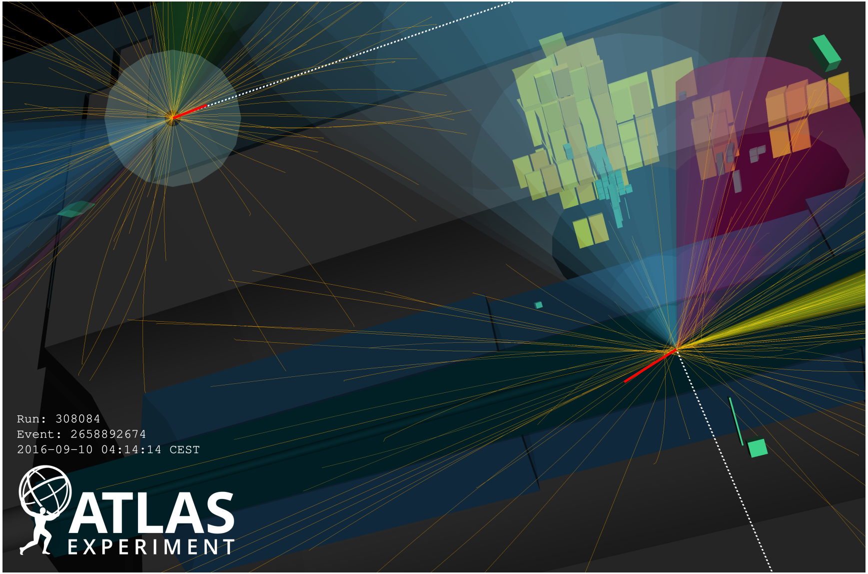

Stopped particles additional material

Dataset and triggers

Data sample (purpose)	**Bunch structure**	**Trigger requirements**	**Offline requirements**
Search sample	Empty	HLT jet $p_T > 55$ GeV HLT $E_T^{miss} > 50$ GeV HLT jet $\lvert\eta\rvert < 2.4$	Leading jet $p_T > 90$ GeV Leading jet $\lvert\eta\rvert < 2.4$
Cosmic sample	–	L1 jet $p_T > 12$ GeV	Leading jet $p_T > 90$ GeV Leading jet $\lvert\eta\rvert < 2.4$
Beam-induced background sample	Unpaired	L1 jet $p_T > 12$ GeV or L1 jet $p_T > 50$ GeV	Leading jet $p_T > 90$ GeV Leading jet $\lvert\eta\rvert < 2.4$
Cavern background sample	Empty	Random	–

Signal regions

Region	Data sample	Number of muons	Leading jet p_{T} [GeV]	α	Leading jet w_{ϕ}	Leading jet $\lvert\eta\rvert$
Central signal region						
SRC	Search sample	0	150–300 300–500 > 500	> 0.2	> 0.02	< 0.8
Inclusive signal region						
SRIncl	Search sample	0	150–300 300–500 > 500	> 0.2	> 0.02	< 2.4
Central discovery regions						
DRC-150 DRC-300 DRC-500	Search sample (2018 data only)	0	> 150 > 300 > 500	> 0.2	> 0.02	< 0.8
Inclusive discovery regions						
DRIncl-150 DRIncl-300	Search sample (2018 data only)	0	> 150 > 300	> 0.2	> 0.02	< 2.4

Control regions

Region	Data sample	Number of muons	Leading jet p_{T} [GeV]	α	Leading jet w_{ϕ}	Leading jet $\lvert\eta\rvert$
Central control and normalisation regions						
CRC-cos	Search sample & BIB sample	$\boldsymbol{\geq 1\ (\lvert\eta\rvert < 1.4)}$	> 90	$\boldsymbol{< 0.2}$	> 0.02	
CRC-bib	**BIB sample**	0	> 90	> 0.2	> 0.01	< 0.8
NRC-bib	Search sample	0	**90–150**	> 0.2	> 0.02	
Inclusive control and normalisation regions						
CRIncl-cos	Search sample & BIB sample	$\boldsymbol{\geq 1\ (\lvert\eta\rvert < 1.4)}$	> 90	$\boldsymbol{< 0.2}$	> 0.02	
CRIncl-bib	**BIB sample**	0	> 90	> 0.2	> 0.01	< 2.4
NRIncl-bib	Search sample	0	**90–150**	> 0.2	> 0.02	

Validation regions

Region	Data sample	Number of muons	Leading jet p_{T} [GeV]	α	Leading jet w_ϕ	Leading jet $\lvert\eta\rvert$
Central validation regions						
VRC-α		$\boldsymbol{\geq 1\ (\lvert\eta\rvert < 1.4)}$		> 0.2	> 0.02	
VRC-bib	Search sample	0	> 150	> 0.2	**0.01–0.02**	< 0.8
VRC-w_ϕ		0		$\boldsymbol{< 0.2}$	> 0.02	
Inclusive validation regions						
VRIncl-α		$\boldsymbol{\geq 1\ (\lvert\eta\rvert < 1.4)}$		> 0.2	> 0.02	
VRIncl-bib	Search sample	0	> 150	> 0.2	**0.01–0.02**	< 2.4
VRIncl-w_ϕ		0		$\boldsymbol{< 0.2}$	> 0.02	
Central BIB normalisation regions						
NRC-α		$\geq 1\ (\lvert\eta\rvert < 1.4)$		> 0.2	> 0.02	
NRC-bib	Search sample	0	**90–150**	> 0.2	0.01–0.02	< 0.8
NRC-w_ϕ		0		< 0.2	> 0.02	
Inclusive BIB normalisation regions						
NRIncl-α		$\geq 1\ (\lvert\eta\rvert < 1.4)$		> 0.2	> 0.02	
NRIncl-bib	Search sample	0	**90–150**	> 0.2	0.01–0.02	< 2.4

SR yields 1

Central signal regions	SRC (2017 data)	SRC (2018 data)
Observed events	92	100
Total expected background events	88 ± 28	119 ± 32
Beam-induced background events	37 ± 23	72 ± 29
Cosmic-ray-induced background events	51 ± 21	47 ± 19
$m(\tilde{g}, \tilde{\chi}_1^0) = (1400, 100)$ GeV	5	6
$m(\tilde{g}, \tilde{\chi}_1^0) = (1400, 900)$ GeV	5	6

Inclusive signal regions	SRIncl (2017 data)	SRIncl (2018 data)
Observed events	239	221
Total expected background events	167 ± 48	208 ± 50
Beam-induced background events	93 ± 42	139 ± 45
Cosmic-ray-induced background events	74 ± 30	69 ± 28
$m(\tilde{g}, \tilde{\chi}_1^0) = (1400, 100)$ GeV	7	9
$m(\tilde{g}, \tilde{\chi}_1^0) = (1400, 900)$ GeV	7	8

SR yields 2

Central discovery regions	Jet p_T > 150 GeV	Jet p_T > 300 GeV	Jet p_T > 500 GeV
Observed events	100	11	4
Total expected background events	119 ± 32	12.5 ± 5.3	4.1 ± 2.3
Beam-induced background events	72 ± 29	2.2 ± 2.1	$0.00^{+0.05}_{-0.00}$
Cosmic-ray-induced background events	47 ± 19	10.3 ± 5.0	4.1 ± 2.3
S^{95}_{exp}	$52.8^{+14.6}_{-13.7}$	$14.3^{+1.4}_{-2.9}$	$7.8^{+4.6}_{-0.2}$
S^{95}_{obs}	45.3	14.1	7.9
CL_B	0.30	0.45	0.56
$p(s=0)$ (Z)	0.5 (0)	0.5 (0)	0.5 (0)

Inclusive discovery regions	Jet p_T > 150 GeV	Jet p_T > 300 GeV	Jet p_T > 500 GeV
Observed events	221	31	11
Total expected background events	208 ± 50	19.7 ± 7.6	6.2 ± 3.4
Beam-induced background events	139 ± 45	4.5 ± 2.3	0.38 ± 0.23
Cosmic-ray-induced background events	69 ± 28	15.2 ± 7.2	5.8 ± 3.4
S^{95}_{exp}	97^{+35}_{-26}	$19.6^{+8.3}_{-5.7}$	$12.7^{+2.3}_{-4.8}$
S^{95}_{obs}	104	29.3	15.5